SPACECRAFT DISINTEGRATION DURING UNCONTROLLED ATMOSPHERIC RE-ENTRY

B. Fritsche[1], T. Roberts[2], M. Romay[3], M. Ivanov[4], E. Grinberg[5], H. Klinkrad[6]

[1]Hypersonic Technology Göttingen, D-37191 Katlenburg-Lindau, Germany
[2]Fluid Gravity Engineering, Liphook, Hampshire GU30 7AZ, U.K.
[3]Grupo de Mecanica del Vuelo, E-28760 Madrid, Spain
[4]Institute for Theoretical and Applied Mechanics, Novosibirsk, 630090 Russia
[5]Energocosmos, Moskow, 115230 Russia
[6]ESOC, D-64293 Darmstadt, Germany

ABSTRACT

Our project group is currently dealing with the problem of uncontrolled re-entry of spacecrafts in the frame of an ESOC contract. The goal is to develop a software system which can be used to predict disintegration of uncontrolled spacecrafts and to calculate the dispersion of its fragments. A full analysis has to consider many different problem fields like flight dynamics, aerodynamics, thermal and structural analysis. We are considering all these fields, but have used simplified approaches to keep the effort for a complete disintegration analysis within acceptable limits. In this paper our theoretical approach is presented. In addition, main features of our analysis software system are discussed and some preliminary results of functional software tests are shown. It is now possible to calculate the trajectory of a spacecraft up to the point where a destruction is detected. The fragmentation process will be treated as next step.

1. INTRODUCTION

Controlled re-entry vehicles like the space shuttle are designed to minimise and withstand the structural and thermal heat loads during return from space to ground. Other objects like rocket stages and space debris enter the dense atmosphere in an uncontrolled manner. Usually these objects burn up during re-entry, but very heavy or compact ones or parts of them may survive and reach ground, which was the case for several re-entering space stations like Skylab or Kosmos 1686 or, just recently, for a Delta rocket body. Fortunately these parts fell down up to now only in thinly populated regions, but for the future with the steady increasing number of space objects and possible candidates for ground impact a means for predicting their trajectory, disintegration and fragmentation is demanded. This is especially true for old satellites equipped with nuclear reactors. For spacecrafts with at least limited controlability like satellites with control thrusters a disintegration prediction tool could give recommendations regarding the controlled choice of entry conditions, if the object shall be de-orbited after completion of its mission.

A theoretical treatment of spacecraft disintegration during uncontrolled re-entry must

- consider possible destruction mechanisms during re-entry
- compute the trajectory and attitude motion of the S/C and its fragments.

As main destruction mechanisms were identified

- Destruction by heating (melting, evaporation)
- Destruction by forces (fracture of joints, deformation)

These destruction mechanisms are considered during calculation of thermal and mechanical loads in the thermal and structural analysis modules respectively.

2. THEORETICAL APPROACH

2.1 Flight dynamic model

The trajectory and attitude motion of each tracked space object is determined by numerical integration of the 6 dof equations of motion

$$\frac{d}{dt}\left(m\vec{V}\right) = \vec{F}_{ext} \qquad (1)$$

$$\frac{d}{dt}\left(I\vec{\omega}\right) = \vec{M}_{ext} \qquad (2)$$

with following assumptions/methods

- External forces and torques are due to gravitation (earth, sun, moon) and surface forces (aerodynamic and solar radiation pressure/shear stress).
- Masses and inertia moments are constant for each object.

- Integration with Runge Kutta method 4th/8th order with fixed/variable step size.
- Trajectory integration in inertial system, attitude calculation in body fixed coordinates.
- Rotation angles formulated in quaternions.
- Uncontrolled re-entry (no thrust).

The complete equations of motion as treated by the calculation are

$$\dot{\vec{R}} = \vec{V} \tag{3}$$

$$m\,\dot{\vec{V}} = m\,\vec{a}_g + \vec{F}_a + \vec{F}_s \tag{4}$$

$$\dot{\vec{q}} = \frac{1}{2} Q\,\vec{\omega} \tag{5}$$

$$I\,\dot{\vec{\omega}} = \vec{M}_g + \vec{M}_a + \vec{M}_s - \vec{\omega} \times I\,\vec{\omega} \tag{6}$$

The environment is modelled with GEM 10B for earth gravitation, central field for sun and moon gravitation and MSIS90E atmosphere for free stream conditions. Surface forces are provided by the aerodynamic model.

2.2 Aerodynamic model

The free stream conditions for re-entry trajectories are known to be hypersonic. The flow velocity decreases during descent and will eventually become subsonic, but this occurs well below the range of maximum heat and mechanical loads and thus the disintegration domain. For disintegration and dispersion analysis some hypersonic approximations can be utilized for the aerodynamic model. With regard to the density the free stream conditions vary from free molecular at altitudes above about 150 km to continuum below say 70 km, depending on the size of the space object. These flow regimes require different theoretical treatment.

The aerodynamics enters the equations of motion (4,6) on the right hand side as part of the external forces and moments. Aerodynamic force and torque are the resulting action of pressure and shear stress distribution over the space object's surface

$$\vec{F}_a = \int_S (p\,\vec{n} + \tau\,\vec{t})dS \tag{7}$$

$$= q_\infty \int_S (c_p\,\vec{n} + c_\tau\,\vec{t})dS \tag{8}$$

$$\vec{M}_a = \int_S (\vec{r} \times p\,\vec{n} + \vec{r} \times \tau\,\vec{t})dS \tag{9}$$

$$= q_\infty \int_S (\vec{r} \times c_p\,\vec{n} + \vec{r} \times c_\tau\,\vec{t})dS \tag{10}$$

$q_\infty = \rho V^2/2$ denotes the dynamic free stream pressure, $c_p = p/q_\infty$, $c_\tau = \tau/q_\infty$ are the local pressure and shear stress coefficients, $\vec{n}$, $\vec{t}$ are surface unit normal and tangential vector on local surface element dS. $\vec{r}$ is the vector distance to the moment reference point, which will be the center of mass (cm) in most cases.

Free molecular regime

If the Schaaf-Chambre formulation for the gas-surface interaction with accommodation coefficients σ_N, σ_T is used and other interactions like catalysis and chemical reactions are ignored, the local aerodynamic coefficients in free molecular flow are in general given by

$$c_{p,F} = \frac{\sigma_N}{\sqrt{\pi} S_\infty^2} \left[\frac{2-\sigma_N}{\sigma_N} \Pi(S_n) + \frac{1}{2} \sqrt{\frac{T_W}{T_\infty}} \chi(S_n) \right] \tag{11}$$

$$c_{\tau,F} = \frac{\sigma_T}{\sqrt{\pi} S_\infty} \sin\Theta\,\chi(S_n) \tag{12}$$

with the speed ratio $S_\infty = Ma\sqrt{\kappa/2}$, its component $S_n = S_\infty \cos\Theta$ normal to the surface element.

Continuum regime

In continuum flow the local aerodynamic coefficients are calculated according to a modified Newtonian theory:

$$c_{p,C} = k_{N1}(\kappa, Ma, \Theta) \cdot \cos^2\Theta + k_{N2}(\kappa, Ma, \Theta) \tag{13}$$

$$c_{\tau,C} = 0 \tag{14}$$

Transition regime

The aerodynamic coefficients in the transition regime are calculated with a local bridging formula

$$c_p = c_{p,C} + (c_{p,F} - c_{p,C}) \cdot f_p(Kn) \tag{15}$$

$$c_\tau = c_{\tau,C} + (c_{\tau,F} - c_{\tau,C}) \cdot f_\tau(Kn) \tag{16}$$

with $0 \le f_{p,\tau} \le 1$.

Shadowing

Above given formulae are valid or can be modified to be valid also on leeside surfaces. However, they cannot be applied to surfaces shadowed by other parts of the spacecraft. According to the hypersonic approximation the shadowed parts of the spacecraft are determined in the aerodynamic analysis by calculating the geometric shadow of all surface elements in a plane perpendicular to the flow velocity and checking mutual shadowing by comparing the distance to the shadow plane in case of overlapping shadows. For shadowed parts of the surface the aerodynamic coefficients are set to zero.

Solar radiation forces

Solar radiation force and torque can be calculated similar to the corresponding aerodynamic quantities in (7,9), if the dynamic pressure is substituted by the solar pressure constant ($\approx 4 \cdot 10^{-6}$ Pa). Pressure and shear stress coefficients depend only on the photon-surface interaction law used.

2.3 Thermal analysis

The thermal analysis consists of two parts. The aerothermal analysis predicts the convective heat transfer to the outer surface of the space object based on the aerodynamic and free stream conditions provided by the aerodynamic and flight dynamic calculation, respectively. Using the calculated heat transfer values the thermal analysis predicts the temperature changes at all positions on the inner and outer surfaces of the object.

2.3.1 Aerodynamic heating

Like the aerodynamic coefficients the heat transfer at a given altitude is computed as a combination of the free molecular and continuum values.

Free molecular regime

The free molecular heat transfer is given by

$$q_F(\theta) = \sigma_E\, p_\infty \sqrt{\frac{RT_\infty}{2\pi}} \left[\left(S_\infty^2 + \frac{\gamma}{\gamma-1} - \frac{(\gamma+1)T_W}{2(\gamma-1)T_\infty}\right)\chi(S_n) - \frac{1}{2}e^{-S_n^2}\right] \tag{17}$$

Continuum regime

In the continuum limit the laminar and turbulent heat transfer formulations as proposed by Detra and Hidalgo and others are used (Ref. 1).

For laminar stagnation point flow:

$$q_C\sqrt{R} = \text{const}\; V^{3.15}\left(\frac{\rho_\infty}{\rho_{SL}}\right)^{0.5}\left(\frac{H_S - h_W}{H_S - h_{W,300}}\right) \tag{18}$$

For turbulent flows:

$$q_C\, x^{0.2} = \text{const}\; V^{3.18}\left(\frac{\rho_\infty}{\rho_{SL}}\right)^{0.8}\phi(p/p_{St}) \tag{19}$$

A Reynolds number based on local momentum thickness of the boundary layer is used as criterion whether the flow is locally laminar or turbulent. It has the form

$$Re_q = \text{const}\; V^{0.477}\left(\frac{\rho_\infty}{\rho_{SL}}\right)^{0.5076}\psi(p/p_{St}) \tag{20}$$

The flow is assumed to be turbulent for $Re_q > 200$.

General case

In the general case the heat transfer is computed using a Knudsen number bridging function to combine the continuum and free molecular limits

$$q = q_C + (q_F - q_C)\cdot f(Kn) \tag{21}$$

For aerodynamically shadowed parts of the surface the heat transfer is set to zero.

The computed heat transfer q is used to determine the surface temperature T_S using the approximation that the convective heat transfer is equal to the net level of radiation emitted from the surface:

$$q = \epsilon(T_S)\sigma_E(T_S)(T_S^4 - T_\infty^4) \tag{22}$$

Melting

If the computed surface temperature exceeds the melting temperature the surface material is assumed to melt. Then the surface temperature remains constant and the convective heat will be transferred in latent heat of melting. It is assumed that the wall melts in a layer growing from the outer surface inside. The rate of growth for the layer thickness is then

$$\dot{s} = q/(H_{melt} - H_W) \tag{23}$$

It is assumed that when the material melts the space object retains its structure and that the geometry remains unchanged until some form of destruction occurs.

2.3.2 Internal heating

The heat transfer from the external to the internal surfaces through the walls is considered only in one dimension. To avoid a finite element approach the time variation of the temperature T_i at the inner end of a thermal joint of length L is computed according to Mezines (Ref. 2) as function of the temperature at the outer end T_o and flight time t

$$\ln\left(1 - \frac{T_i}{T_o}\right) = -2.42\alpha\left(\frac{0.473}{\eta + 0.473}\right)\frac{t}{L^2} + 0.214 \tag{24}$$

In addition to heat conduction in the interior radiative heat exchange via greybody radiation is considered.

2.4 Structural analysis

Even simple objects can be deformed in complicated ways during re-entry. A full structural analysis would require correspondingly complicated, time-consuming analysis methods. The analysis used in the present approach is much simplified and restricted to fracture of joints between some elementary parts of the space object. The main advantage besides much higher computation performance is the easy way of setting up the structural model even for complicated geometries.

The elementary terms of the structural analysis are sections and joints. A joint is an element connecting other elements and which will be considered in the structural analysis. A section is a cut plane through one or more joints.

The stresses at any point of the section with coordinates (y,z) are determined by

$$\sigma = \frac{F_x}{A} + \frac{M_y z}{J_y} + \frac{M_z y}{J_z} \tag{25}$$

$$\tau = \frac{M_x \cdot \rho}{J_\rho} \tag{26}$$

where A = total cross section of all joints in the section, J_y, J_z are the (area) moments of inertia of all joints and F_x, M_x, M_y, M_z are integral loads in the section (force and moments). From σ and τ the equivalent stress $\sigma_{eq} = \sqrt{\sigma^2 + 3\tau^2}$ is derived.

A joint is considered to be destroyed if the equivalent stress exceeds its breaking stress. The breaking stress is a function of the averaged joint temperature. This temperature is provided by the thermal model. The actual stress depends on the forces and moments acting on the joint. These quantities are determined by surface forces acting on the geometric part cut off by the section and inertial forces. They are provided by the aerodynamic and the flight dynamic model respectively.

3. SOFTWARE SYSTEM

3.1 Calculation modules

Each model was realized in a separate software module, written in Fortran. There are four different analysis modules: flight dynamic module, aerodynamic module, thermal module, structural module. These modules were developed independent from each other after specifying the I/O interfaces between the modules. As indicated in the model descriptions the flight dynamics gets information from aerodynamics, aerodynamics gets information from flight dynamics and thermal analysis, thermal analysis gets information from flight dynamics and aerodynamics. The structural analysis gets information from all other modules but returns nothing.

3.2 Geometry module

All modules need some description of the spacecraft geometry. This is provided by a separate geometry module. With this module the S/C geometry is constructed from elementary geometric objects (primitives) like rectangles, circles, cones and spheres. As intermediate step primitives are grouped together to build a compound. These compounds are combined to build compounds of higher levels until the complete spacecraft is constructed. The compound and element structure is essential to the concept of modelling an object in the software.

For modules which perform surface integrations like aerodynamic and thermal module a panelized surface description of each primitive is provided as well. The surface integrals are calculated in the software as sums over all relevant panels. Local flow inclination angles are calculated with the panel surface normal vectors.

3.3 Model definition

Each model works with certain parameters, like mass, inertia moment, reference quantities. These parameters are specified in the model definition module after selecting or building a geometry with the geometry module. Some values are relevant only for the whole spacecraft, others have to be defined for each element.

3.4 Material subsystem

At the stage of model construction the surface material dependent properties are not specified explicitly. Instead a predefined material name is selected. The material properties, which can be temperature dependent, are determined in the calculation modules at run time by calling special subroutines, added to the modules at code linking. These subroutines read the material properties from material data files, created by the material data module. The material data are input by the user (taken from material data books) during a run of this module prior to the use of the corresponding data.

3.5 System manager

The system manager is the main user interface. This program is called SCARAB for 'SpaceCraft Atmospheric Re-entry and Aerothermal Break-up'. It presents a main menu from which a complete calculation can be performed, including pre- and postprocessing. The menu consists of four subwindows. The first serves for preprocessing. From here the geometry module and the model definition module can be called. Also some additional initial data not provided by other modules are specified here. The second window selects the calculation chain. This chain specifies the order in which the calculation modules are called. The number of calls is specified a third window. Fig. 1 illustrates the chaining concept.

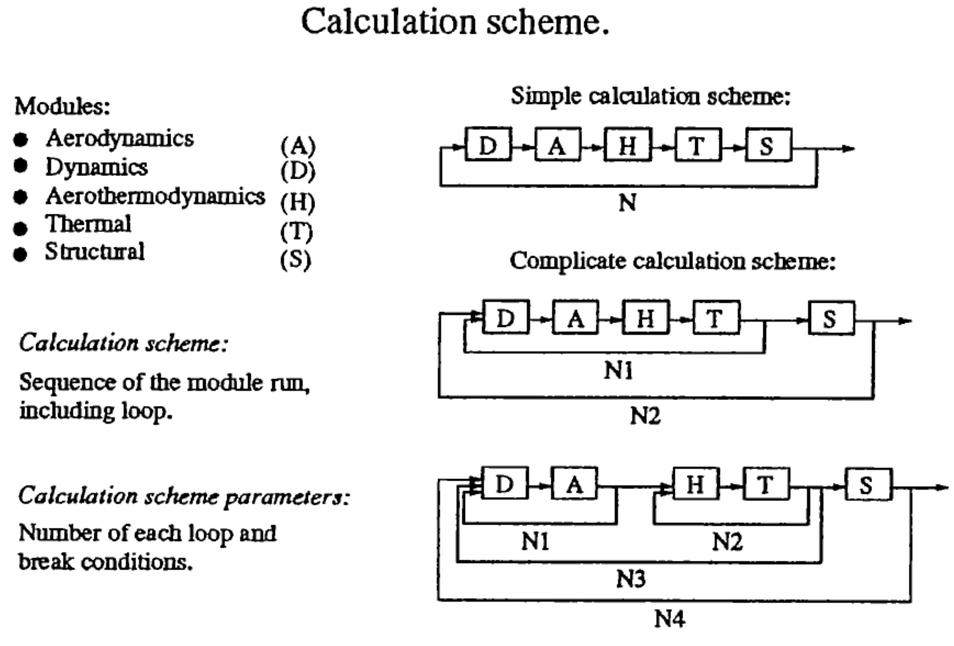

Figure 1: Examples of different calculation chains.

The forth window lists all output file produced by the modules during calculation. These files contain module interface data, surface distributions, data histories and status files. The surface distributions can be visualized as color map on the panelized spacecraft geometry as created by the geometry module.

4. TEST RESULTS

The software functionality was verified with some simple shaped satellites. Figure 2 shows as example a calculated temperature distribution on a Mirka shaped satellite (sphere with cylindrical ring on the rear side, to be launched this year). The stagnation temperature is about 830 K. Pressure, shear stress and heat flux distributions look similar for this case (flight altitude of 120 km, nearly free molecular flow).

Surface materials with a melting temperature below 830 K will start to melt in the stagnation region. This is shown in Figure 3. An initial pitch angle of 30 deg. was assumed. The mass distribution in the satellite was specified to stabilize the attitude motion (center of mass upstream of center of pressure). Therefore the satellite oscillates around its stable attitude and the melting region is smeared out in a pitching angle range of $\pm 30°$ (initially).

Starting at 120 km altitude and with pitch angle of 30° the re-entry motion was calculated. Figure 4 shows the time development of the pitch angle. Figure 5 shows the calculated flight altitude. For this re-entry calculation the thermal analysis was excluded from the calculation chain.

The attitude motion calculation was a severe test for the flight dynamic module and also for its strongly coupled aerodynamic module. At the maximum of aerodynamic moments the integration time step had to be reduced to about 0.03 s to follow the fast oscillation of the satellite's attitude angles.

The pitch angle in Figure 4 is defined as the rotation angle about the orbital axis of the satellite. The rise of the pitch angle near the end of the trajectory is due to the increasing flight path angle γ, which is followed by the pitch angle due to the aerodynamic stabilisation.

Another test satellite is shown in Figure 6.

This satellite was also started numerically at 120 km altitude, but with attack angles all being zero. The center of mass of this satellite is located downstream of the center of pressure and this attitude is unstable. The pitch angle will increase with time and the satellite will eventually turn around. Figure 7 shows the actual and the breaking stress in one of the joints connecting the solar panels to the central cylinder.

The breaking stress decreases slowly due to increasing temperature, whereas the actual stress increases due to the rising attack angle of the panels, reaching its maximum value at $\alpha = 90°$. The calculation was stopped by the thermal module after 110 seconds, since the solar panels were detected to be completely melted (A panel material with low melting point was selected. The same calculation with low melting joint material resulted in a program stop caused by the structural module, which detected the joint to be broken due to vanishing breaking stress near the melting point).

Figure 8 shows the temperature distribution on the leeside. In this picture one can identify the aerodynamic shadow cast by the front disk on the central cylinder. The solar panels are still solid on this side.

5. CONCLUSIONS

The project status can be summarized as follows: The analysis modules are operating together in calculation chains. The definition of geometric and physical parameters for a desired spacecraft model is easily carried out with the system manager and its cooperating modules. The trajectory and attitude motion can be predicted up to the point where either the thermal or the structural module detect a destruction. For a calculation chain containing only the flight dynamic and aerodynamic modules this restriction does not apply. However, the flight altitude usually must not become negative. This would be a stopping condition caused by the flight dynamics module.

The next task will be the prediction of trajectory and attitude motion for the fragments generated due to the destruction event. There are already features implemented in the system manager to assist the user in this work.

6. REFERENCES

1. Detra, N. L. and Hidalgo, H., *Generalised Heat Transfer Formulas and Graphs of Nose Cone Re-Entry Into the Atmosphere*, ARS Journal, Vol. 31, 318–321, 1961.

2. Mezines, S. A., *A Semi-Empirical Method for Correlating the Thermal Performance of Charring Ablative Materials*, AIAA Paper 68-757.

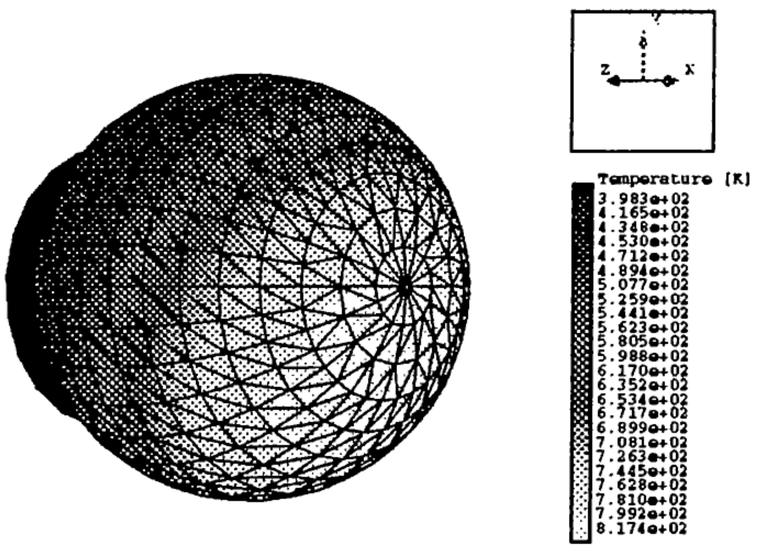

Figure 2: Temperature distribution on Mirka shaped satellite.

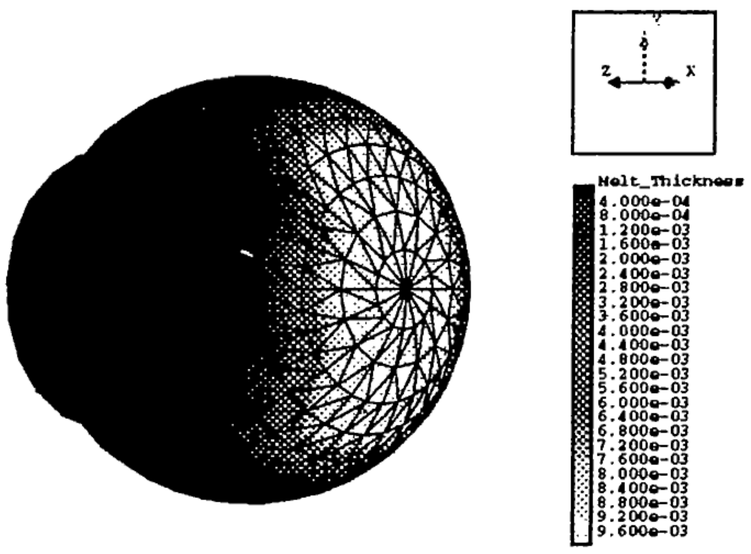

Figure 3: Stagnation region melting on Mirka shaped satellite (Melt thickness in m).

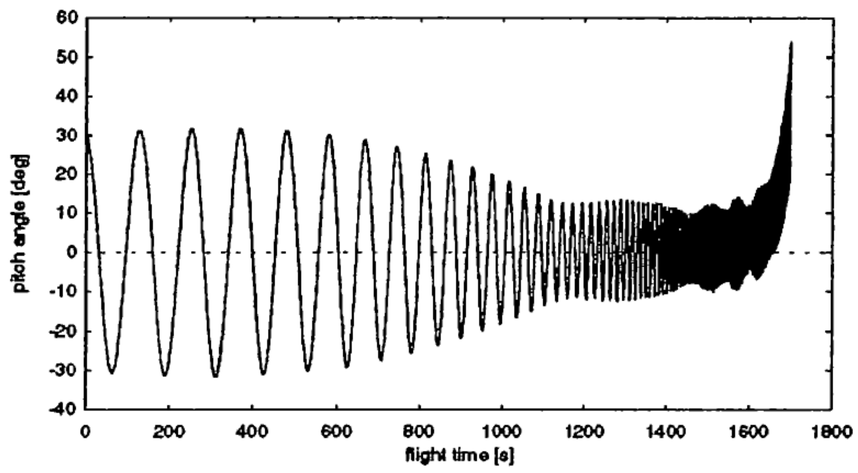

Figure 4: Pitch angle during re-entry.

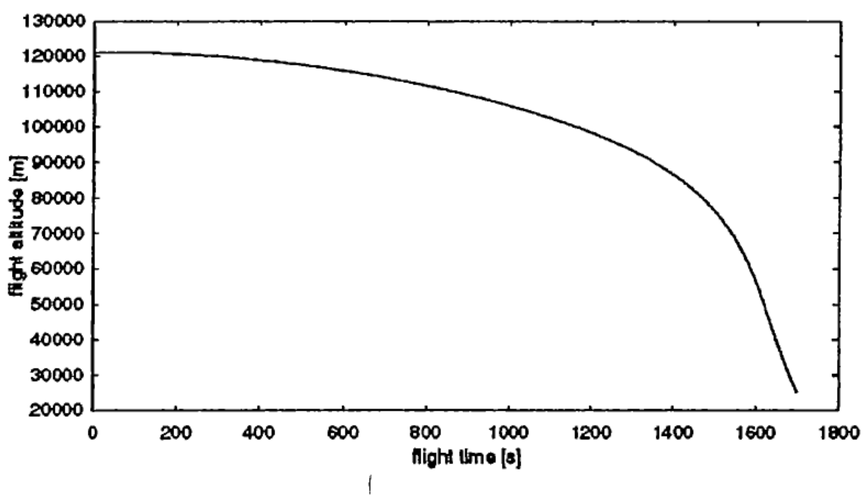

Figure 5: Flight altitude during re-entry.

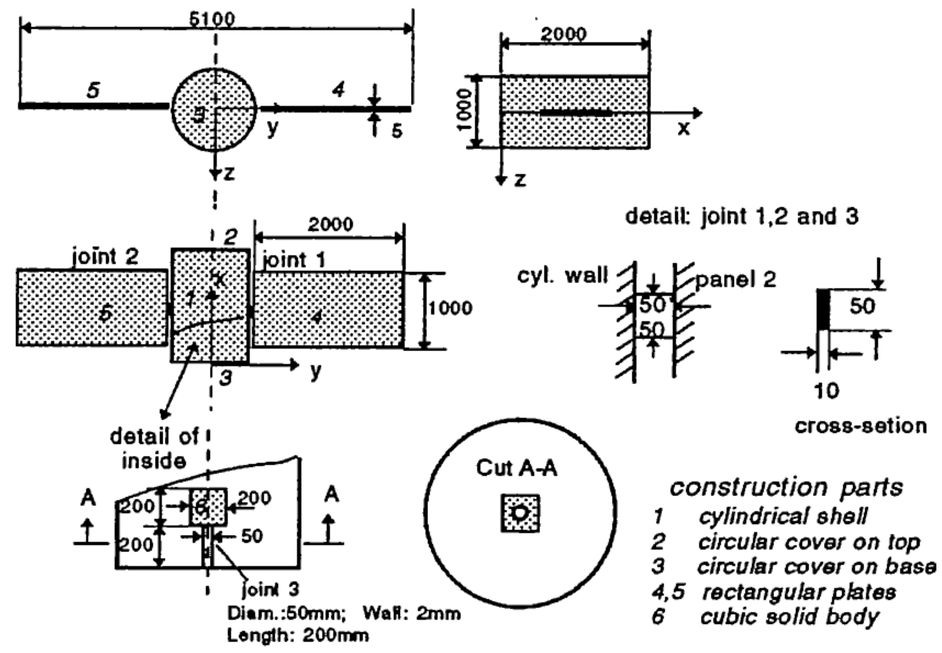

Figure 6: Sketch of test case satellite.

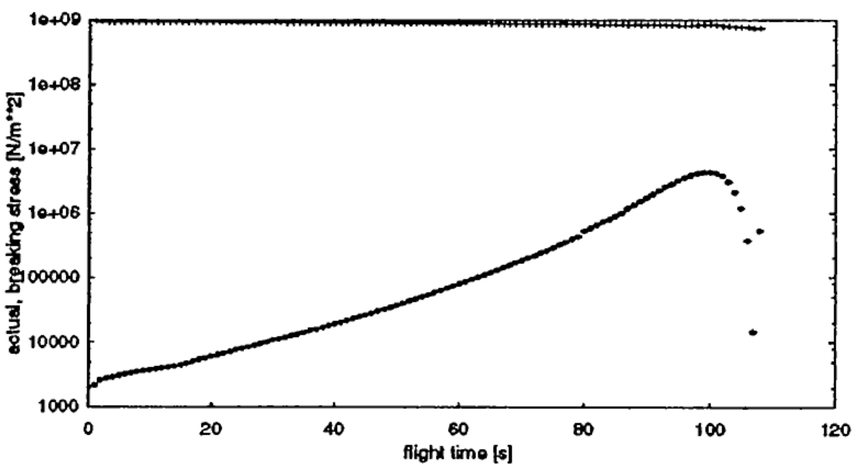

Figure 7: Calculated stresses for test case.

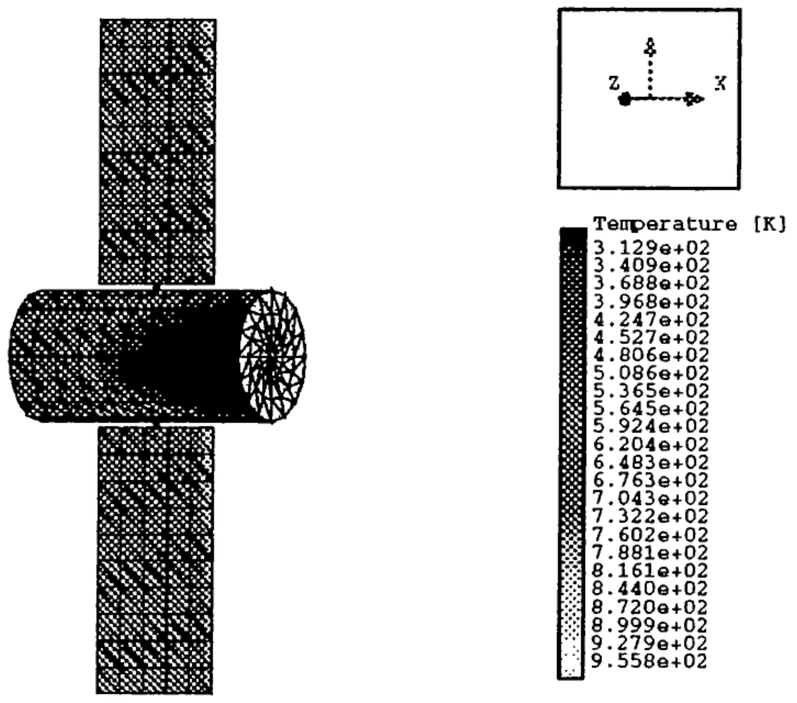

Figure 8: Temperature distribution on the test satellite.

Chapter 8

Risk Analysis and Damage Assessment